

Electronic Supplementary Information for the manuscript entitled:

High-Performance Reverse Osmosis Nanocomposite Membranes Containing the Mixture of Carbon Nanotubes and Graphene Oxides

*Hee Joong Kim, Min-Young Lim, Kyung Hwa Jung, Dong-Gyun Kim,[†] Jong-Chan Lee**

School of Chemical and Biological Engineering and Institute of Chemical Process, Seoul
National University, 599 Gwanak-ro, Gwanak-gu, Seoul 151-742, Republic of Korea

KEYWORDS: high water flux, reverse osmosis, carbon nanotubes, graphene oxides, water
purification

1. ESR analysis

To observe the radical scavenging activity of CNTa and GO, ESR spectra were recorded during the active chlorine exposure to membrane active layers. Figure S13 shows the ESR spectra of the sodium hypochlorite solution containing membrane active layers with time. These spectra were characteristics for DMPO-OOH radical adducts and/or DMPO-OH. Although the resolution was not clear due to the resonance of hydroxyl groups, the characteristic peaks can be obviously observed. The intensity of ESR spectrum for the active layer of PA membrane decreased slightly after 2 h of chlorine exposure, while those for the active layers of PA membrane with carbon nanomaterials decreased more. In particular, the ESR intensity of the PA-CNTa/GO membrane was strongly reduced due to the large radical scavenging effect of CNTa and GO. Figure S14 shows the time-dependant relative ESR intensity changes during the chlorine exposure to membrane active layers. It was found that the radical scavenging behavior was strongly related to the chlorine resistance properties of the membranes. Therefore, the chlorine resistance properties of PA-CNTa/GO membrane mainly originated from the antioxidant ability of the CNTa and GO.

Table S1. XPS elemental composition (at%) and O/C ratio of pristine CNT, CNTa, graphite, and GO.

	C contents	O contents	O/C ratio
Pristine CNT	93.02	6.98	0.075
CNTa	75.87	24.13	0.318
Graphite	89.12	10.88	0.122
GO	68.14	31.86	0.468

Table S2. Water flux and salt rejection values of the membranes prepared in 2 and 3 wt% of MPD (PA-CNT, PA –GO membrane were prepared with 0.001 wt% of CNT and GO in aqueous solution, respectively and PA-CNT/GO membrane was prepared with 0.02 wt% of CNT/GO mixture in aqueous solution, the membranes were tested by cross-flow filtration, 2000 ppm NaCl solution as a feed solution, 15.5 bar of feed pressure, and 500 mL min⁻¹ of flow rate).

	MPD wt%	Water flux [LMH]	Salt Rejection [%]
PA	2	34.00 ± 0.67	96.63 ± 1.34
	3	32.63 ± 1.68	96.48 ± 0.44
PA-CNT	2	40.84 ± 1.84	96.22 ± 0.67
	3	44.23 ± 2.35	96.75 ± 0.49
PA-GO	2	36.68 ± 0.98	96.28 ± 0.83
	3	38.19 ± 1.44	96.96 ± 0.58
PA-CNT/GO	2	53.25 ± 1.88	95.84 ± 0.52
	3	58.96 ± 1.31	96.63 ± 0.65

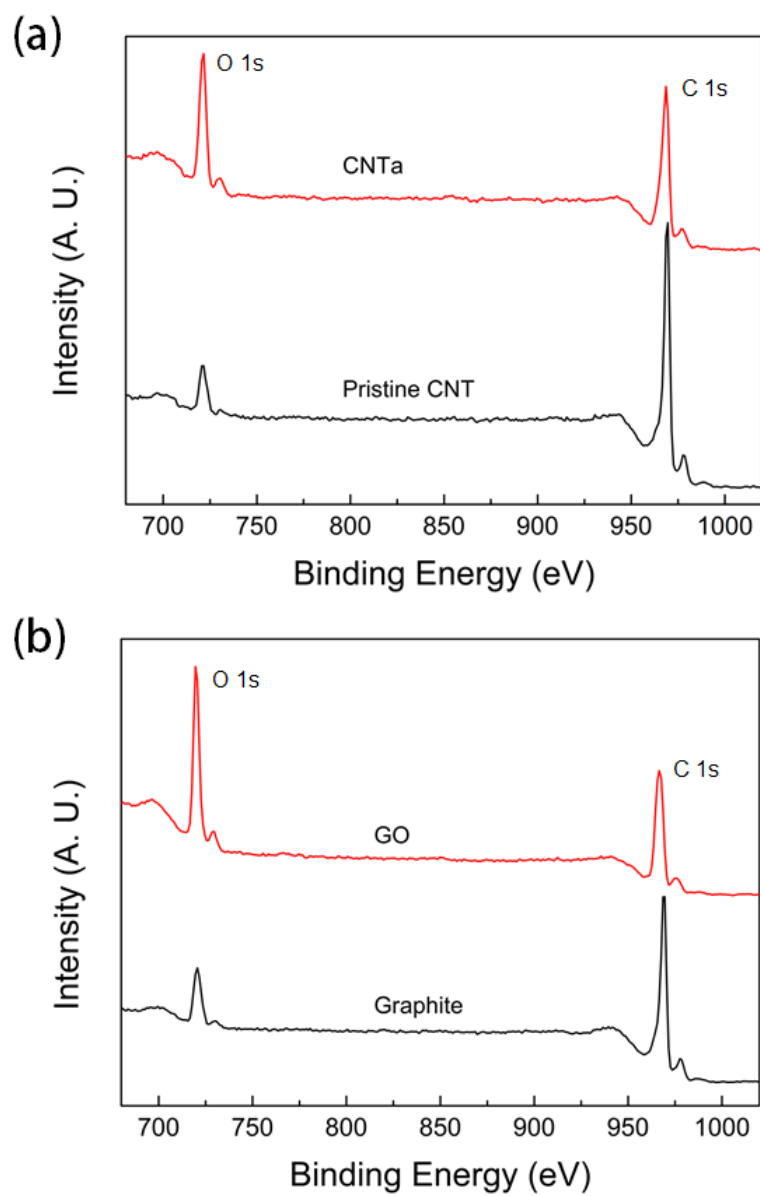


Fig. S1 XPS spectra of (a) pristine CNT and CNTa, and (b) graphite and GO.

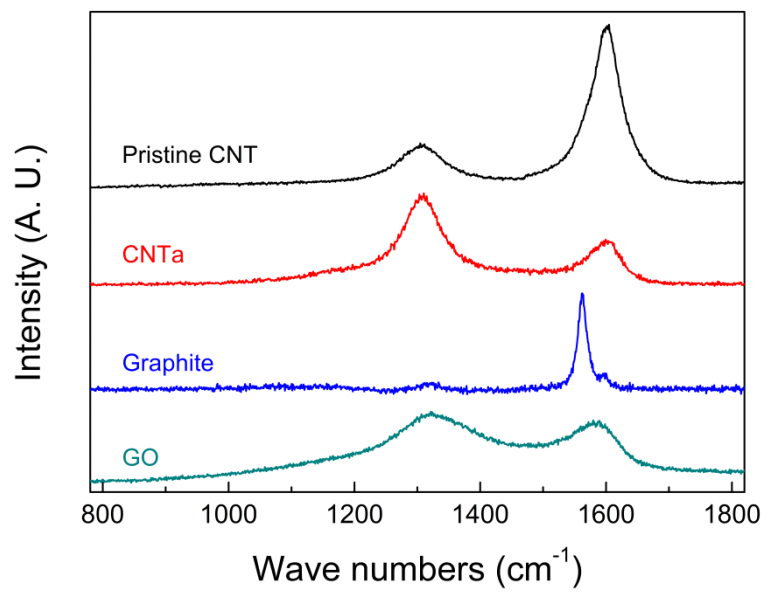


Fig. S2 Raman spectra of pristine CNT, CNTa, graphite, and GO.

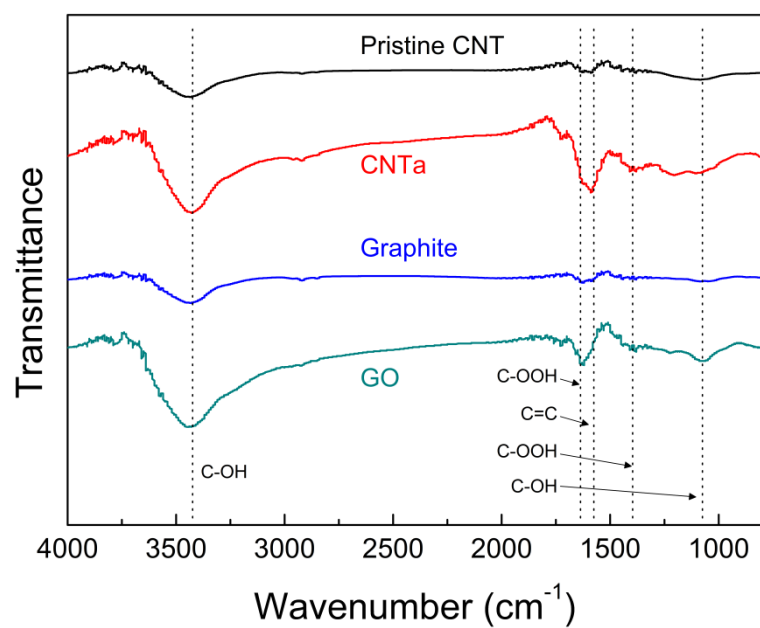


Fig. S3 FT-IR spectra of pristine CNT, CNTa, graphite, and GO.

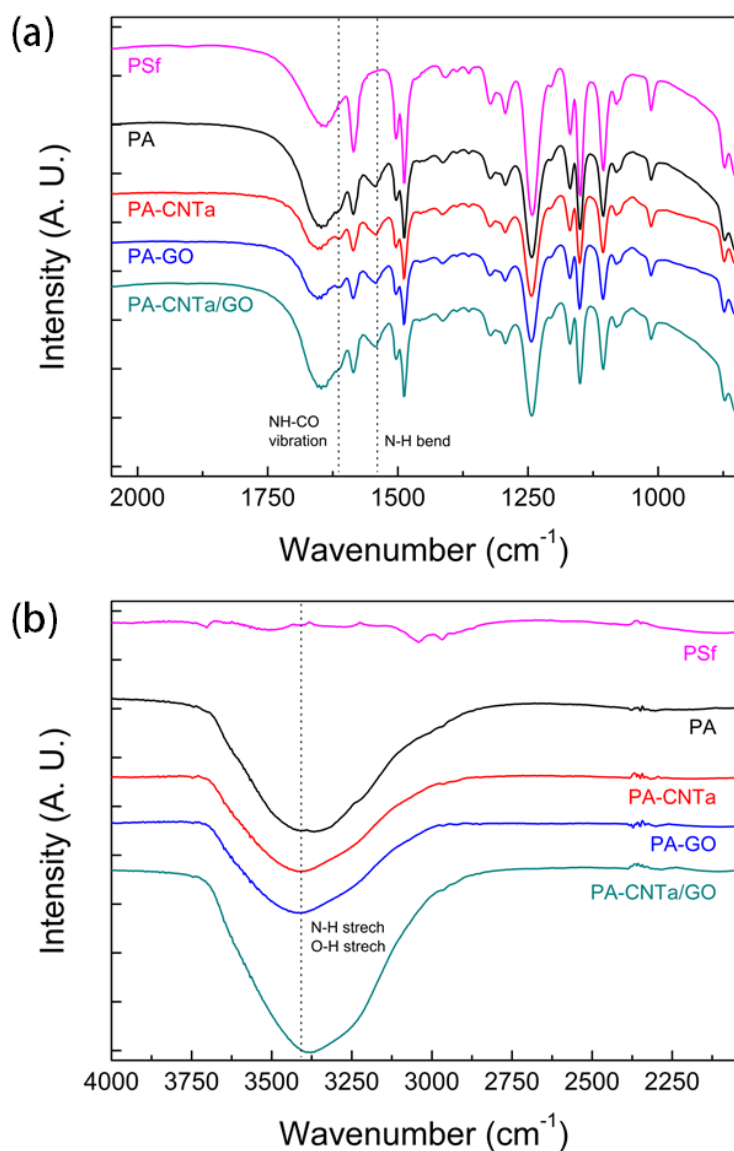


Fig. S4 FT-IR spectra of PSf, PA, PA-CNTa (prepared using the MPD aqueous solution containing 0.001 wt% of CNTa), PA-GO (prepared using the MPD aqueous solution containing 0.001 wt% of GO), and PA-CNTa/GO (prepared using the MPD aqueous solution containing 0.02 wt% of CNTa/GO) membranes; wavenumber at (a) 2050-850 cm^{-1} , and (b) 4000-2050 cm^{-1} .

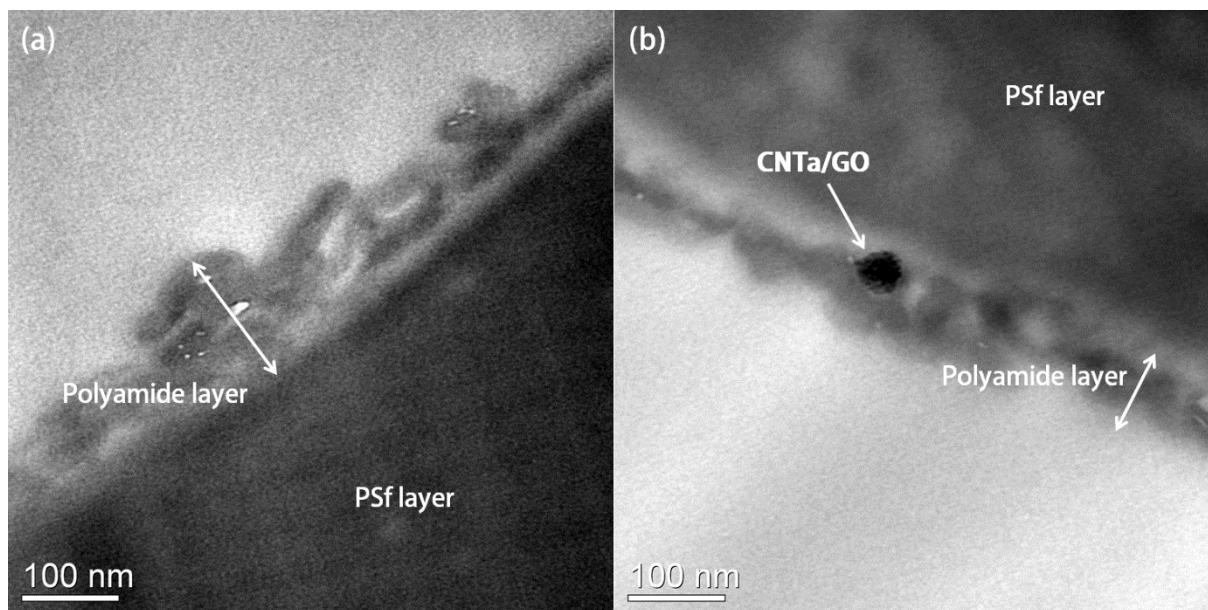


Fig. S5 Cross-sectional TEM images of PA and PA-CNTa/GO (prepared using the MPD aqueous solution containing 0.02 wt% of CNTa/GO) membranes.

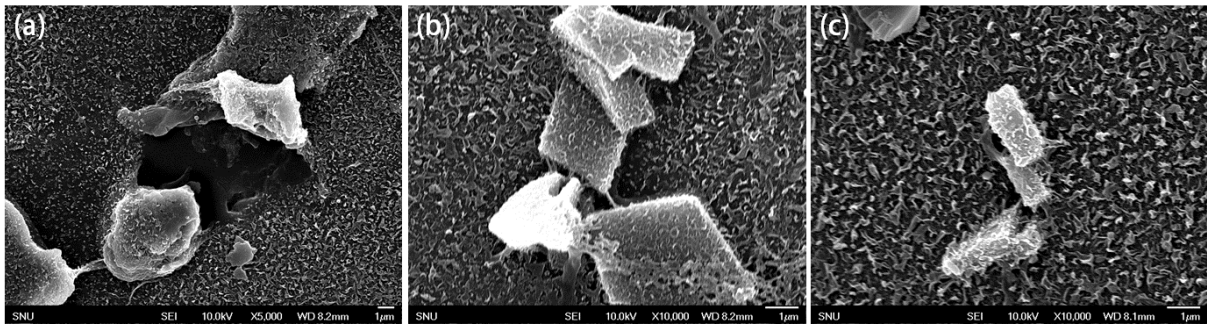


Fig. S6 SEM images at the top surfaces of (a) PA-CNTa (prepared using the MPD aqueous solution containing 0.01 wt% of CNTa), (b) PA-GO (prepared using the MPD aqueous solution containing 0.01 wt% of GO), and (c) PA-CNTa/GO (prepared using the MPD aqueous solution containing 0.03 wt% of CNTa/GO) membranes.

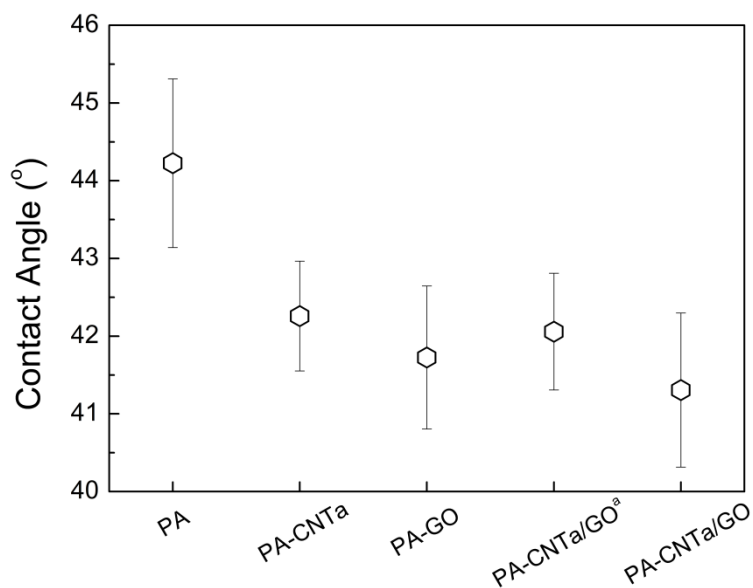


Fig. S7 Contact angle values of PA, PA-CNTa (prepared using the MPD aqueous solution containing 0.001 wt% of CNTa), PA-GO (prepared using the MPD aqueous solution containing 0.001 wt% of GO), PA-CNTa/GO^a (prepared using the MPD aqueous solution containing 0.001 wt% of CNTa/GO), and PA-CNTa/GO (prepared using the MPD aqueous solution containing 0.02 wt% of CNTa/GO) membranes.

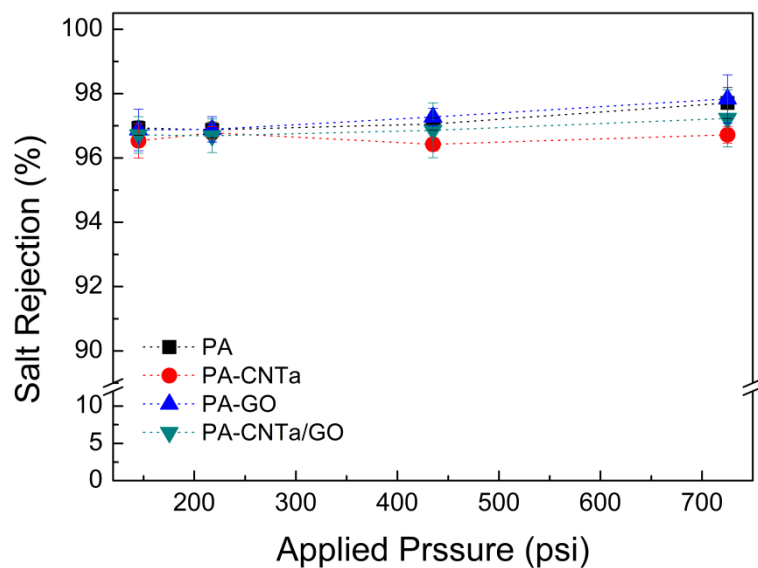


Fig. S8 Salt rejection measurement of the PA, PA-CNTa (prepared using the MPD aqueous solution containing 0.001 wt% of CNTa), PA-GO (prepared using the MPD aqueous solution containing 0.001 wt% of GO), and PA-CNTa/GO (prepared using the MPD aqueous solution containing 0.02 wt% of CNTa/GO) membranes at different applied pressure (tested by cross-flow filtration, 2000 ppm NaCl solution as a feed solution, and 500 mL min⁻¹ of flow rate).

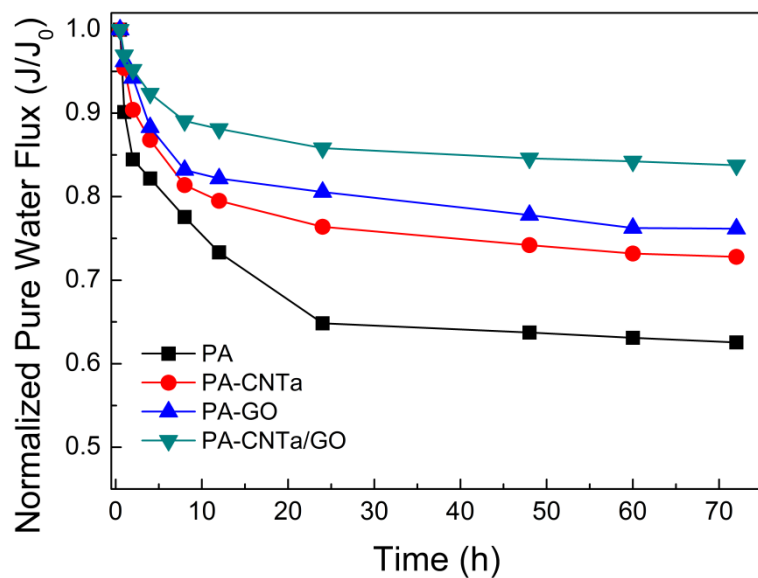


Fig. S9 Normalized pure water flux measurement with time at 50 bar of feed pressure for PA, PA-CNTa (prepared using the MPD aqueous solution containing 0.001 wt% of CNTa), PA-GO (prepared using the MPD aqueous solution containing 0.001 wt% of GO), and PA-CNTa/GO (prepared using the MPD aqueous solution containing 0.02 wt% of CNTa/GO) membranes (tested by cross-flow filtration, and 350 mL min⁻¹ of flow rate).

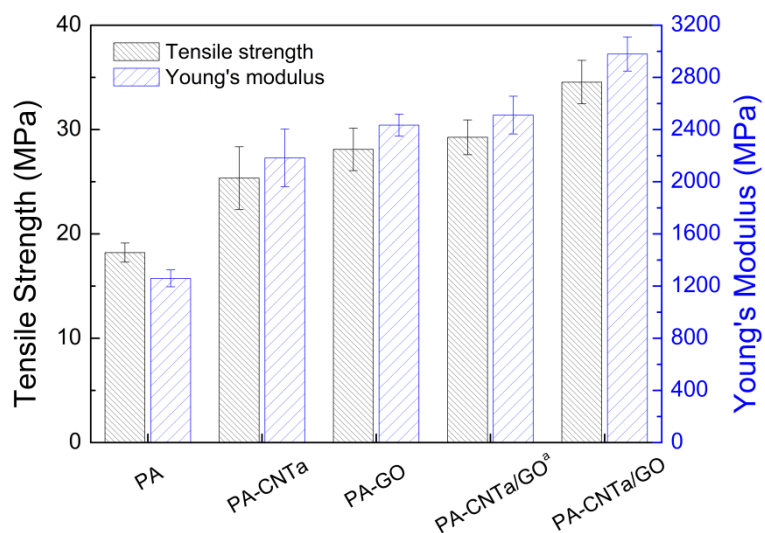
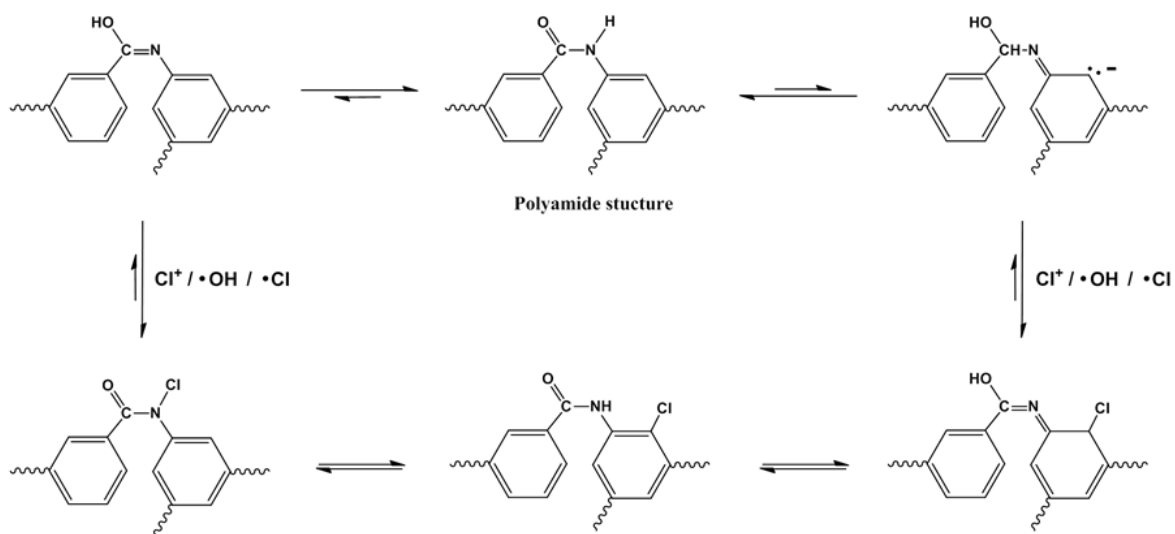


Fig. S10 Mechanical properties of PA, PA-CNTa (prepared using the MPD aqueous solution containing 0.001 wt% of CNTa), PA-GO (prepared using the MPD aqueous solution containing 0.001 wt% of GO), PA-CNTa/GO^a (prepared using the MPD aqueous solution containing 0.001 wt% of CNTa/GO), and PA-CNTa/GO (prepared using the MPD aqueous solution containing 0.02 wt% of CNTa/GO) membranes.

Typical chlorination of polyamide membrane



Antioxidant mechanism of CNT/GO

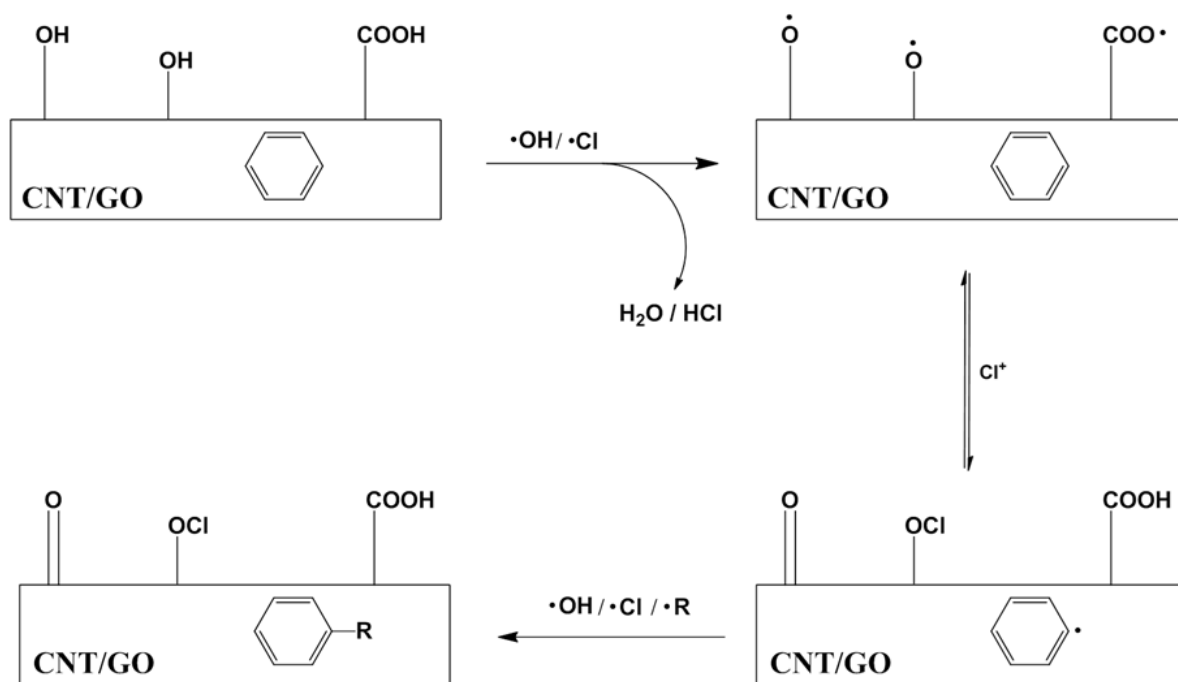


Fig. S11 Typical chlorination of polyamide membrane and antioxidant mechanism of CNT and GO.

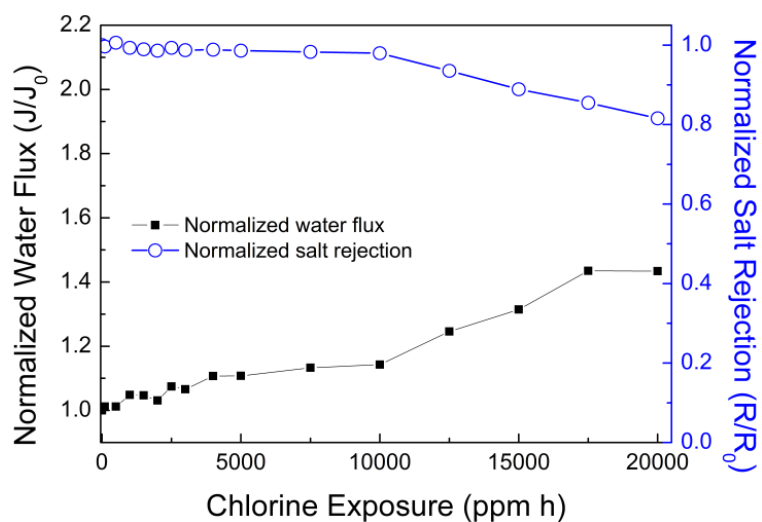


Fig. S12 Membrane performance behaviors under the active chlorine exposures of PA-CNTa/GO membrane prepared using the MPD aqueous solution containing 0.001 wt% of CNTa/GO (tested by cross-flow filtration, after the chlorine exposure using 500 ppm chlorine solution, 2000 ppm NaCl solution as a feed solution, 15.5 bar of feed pressure, and 500 mL min⁻¹ of flow rate).

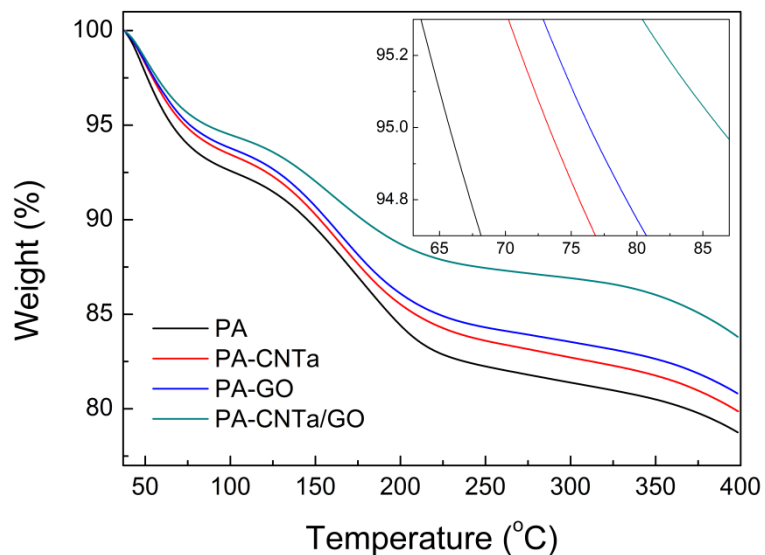


Fig. S13 TGA analysis of the membrane active layers under air; PA, PA-CNTa (prepared using the MPD aqueous solution containing 0.001 wt% of CNTa), PA-GO (prepared using the MPD aqueous solution containing 0.001 wt% of GO), and PA-CNTa/GO (prepared using the MPD aqueous solution containing 0.02 wt% of CNTa/GO) membranes.

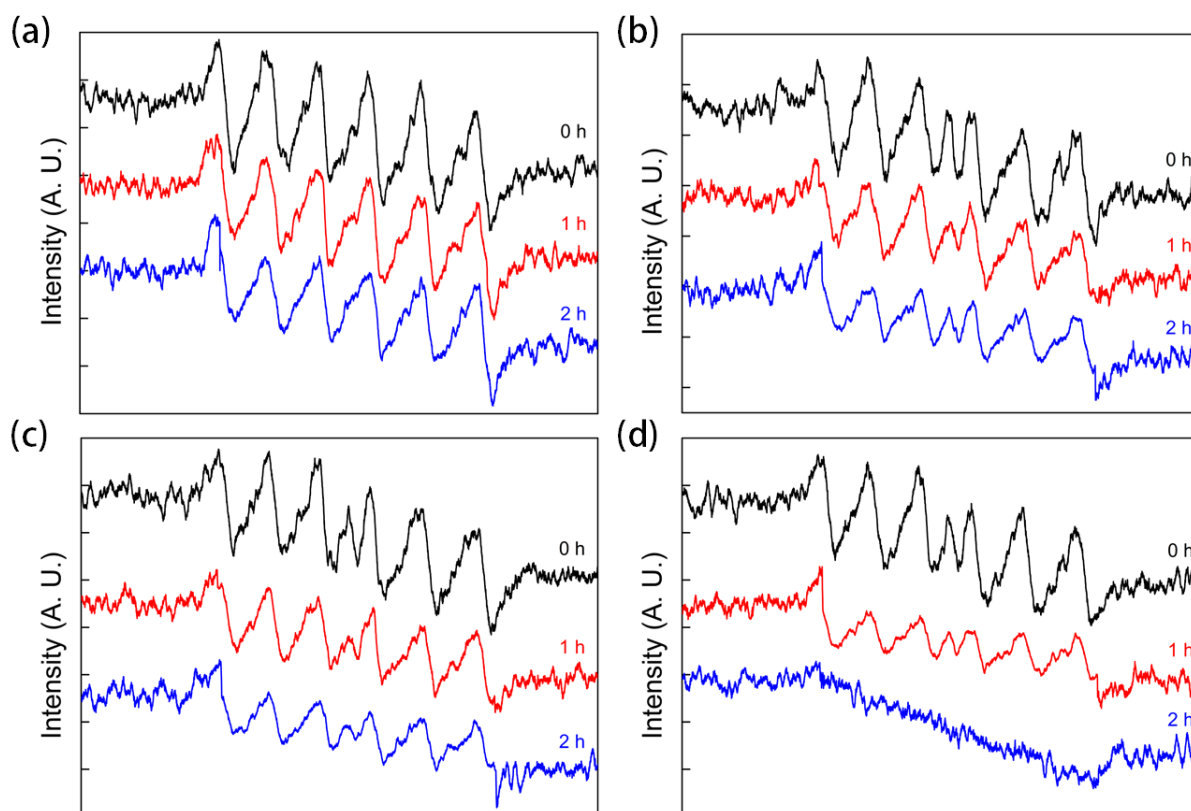


Fig. S14 ESR spectra obtained during the active chlorine exposure to membrane active layers; (a) PA, (b) PA-CNTa (prepared using the MPD aqueous solution containing 0.001 wt% of CNTa), (c) PA-GO (prepared using the MPD aqueous solution containing 0.001 wt% of GO), and (d) PA-CNTa/GO (prepared using the MPD aqueous solution containing 0.02 wt% of CNTa/GO) membranes.

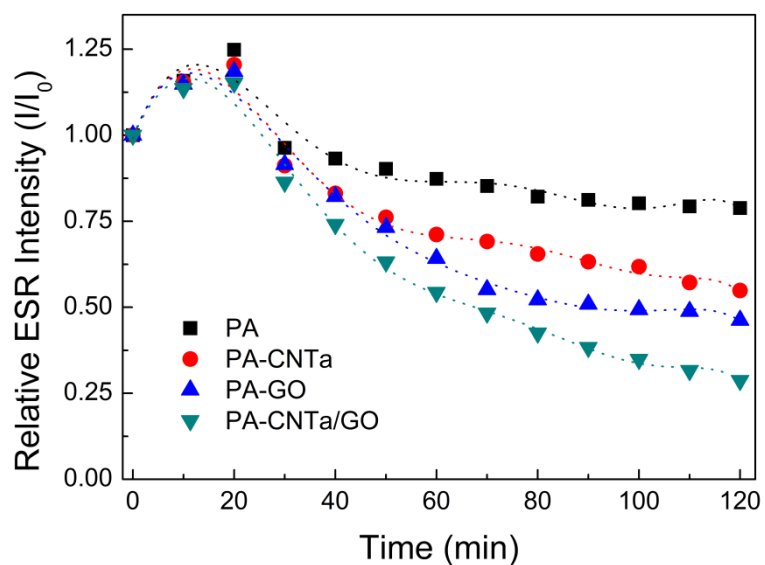


Fig. S15 Time-dependant relative ESR intensity changes during the active chlorine exposure to membrane active layers; PA, PA-CNTa (prepared using the MPD aqueous solution containing 0.001 wt% of CNTa), PA-GO (prepared using the MPD aqueous solution containing 0.001 wt% of GO), and PA-CNTa/GO (prepared using the MPD aqueous solution containing 0.02 wt% of CNTa/GO) membranes.